Petroleum Research 11 (2026) 38–49

Contents lists available at ScienceDirect

Petroleum Research

journal homepage: http://www.keaipublishing.com/en/journals/petroleum-research/

Full Length Article

Investigation of the anionic-zwitterionic and anionic-nonionic surfactant mixtures on enhanced oil recovery using microfluidic devices

Yafei Liu [a,*], Chenyue Ling [a], Yixin Luo [b], Na Liu [c], Gaoxin Li [a], Desheng Zhou [a]

[a] College of Petroleum Engineering, Xi'an Shiyou University, Xi'an, Shaanxi, 710065, China
[b] Shale Oil Development Branch, PetroChina Changqing Oilfield Co., Qingyang, Gansu, 745000, China
[c] No.4 Oil Production Plant, PetroChina Changqing Oilfield Co., Yinchuan, Ningxia, 750006, China

ARTICLE INFO

Article history:
Received 8 April 2025
Received in revised form
21 July 2025
Accepted 23 July 2025
Available online 30 July 2025

Keywords:
Anionic-zwitterionic surfactant mixture
Anionic-nonionic surfactant mixture
Microfluidics
Enhanced oil recovery

ABSTRACT

Surfactant flooding is one of the widely applied enhanced oil recovery methods. However, the application of a single surfactant is often insufficient to meet the demand for oil recovery. Consequently, a variety of surfactant mixtures have been employed to enhance oil recovery efficiency. A comprehensive understanding of the interactions between surfactant mixtures, crude oil, formation water and rock is essential for the effective design and optimization of the surfactant flooding procedures. In this work, anionic-zwitterionic and anionic-nonionic surfactant mixtures with varying compositions were investigated using different microfluidic devices. Single dead-end pore structure that was captured from a real rock pore throat structure was initially employed for a quick screening of the optimum surfactant composition, considering the effect of the presence of connate brine. The selected surfactant compositions were tested using a micromodel with heterogeneous pore-throat network. The results indicate that 0.4 wt% sodium dodecyl benzene sulfonate with 0.6 wt% octadecyl dimethyl betaine and 0.4 wt% sodium dodecyl benzene sulfonate with 0.6 wt% hexyl D-glucoside surfactant mixtures resulted in higher recovery rate in the dead-end pore structure. In the subsequent micromodel experiments, 0.4 wt % sodium dodecyl benzene sulfonate with 0.6 wt% octadecyl dimethyl betaine showed better oil recovery performance. To further explain the oil recovery performance of the surfactant mixtures, interfacial tension, viscoelasticity and critical micelle concentration values were measured and calculated to provide an insight into their interfacial activities. It was observed that anionic-zwitterionic and anionic-nonionic surfactant mixtures displaced oil in different manners attributing to their distinct interfacial properties. The anionic-zwitterionic surfactant mixture primarily displaced the crude oil through solubilization and emulsification due to its lower interfacial tension and critical micelle concentration of the surfactant mixture, whereas the anionic-nonionic surfactant mixture displaced oil through peeling and mobilization as a result of relatively higher interfacial tension and interfacial viscoelasticity.

© 2025 Chinese Petroleum Society. Publishing services by Elsevier B.V. on behalf of KeAi Communications Co. Ltd. This is an open access article under the CC BY-NC-ND license (http://creativecommons.org/licenses/by-nc-nd/4.0/).

1. Introduction

Application of surface active substances is ubiquitous in assorted research fields including food industry, cosmetics, pharmaceuticals, etc. (Fu et al., 2024; Kralova and Sjöblom, 2009; Mulligan et al., 2001; Singh et al., 2007; Vecino et al., 2017). Particularly in the petroleum industry, surface active substances such like surfactants and nanoparticles have been extensively applied during drilling and production process (Jia et al., 2022; Tavakkoli et al., 2022). In the drilling process, surfactants can be used as biocide, foaming agent and emulsifiers (Quintero, 2002). During oil recovery process, surfactants are typically used as oil displacement agents (Hama et al., 2023; Isaac et al., 2022). Application of surfactants could alter the interfacial properties between the oil and aqueous phase and the wettability of the rock

* Corresponding author.
E-mail address: yafliu@xsyu.edu.cn (Y. Liu).
Peer review under the responsibility of Editorial Office of Petroleum Research.

https://doi.org/10.1016/j.ptlrs.2025.07.004
2096-2495/© 2025 Chinese Petroleum Society. Publishing services by Elsevier B.V. on behalf of KeAi Communications Co. Ltd. This is an open access article under the CC BY-NC-ND license (http://creativecommons.org/licenses/by-nc-nd/4.0/).

surface resulting in higher oil recovery (Hirasaki et al., 2011; Bashir et al., 2022).

Surfactants applied to enhance oil recovery are usually categorized as anionic, cationic, nonionic, and zwitterionic surfactants according to the head group charge (Chen and Schechter, 2021; Chowdhury et al., 2022). Commonly applied anionic surfactants include carboxylate, sulfonate, sulfate and phosphate type surfactants based upon its hydrophilic groups (Elraies et al., 2010; Ko et al., 2014; Negin et al., 2017; Zhao et al., 2006). These surfactants exhibit different temperature tolerance and salt resistance depending on the specific functional group. Anionic surfactants are the most widely used surfactants in sandstone reservoirs owing to lower adsorption onto the rock (Bashir et al., 2022; Kamal et al., 2017). Cationic surfactants possess positive charge groups and quaternary ammonium salt type is one of the widely applied cationic surfactants (Bi et al., 2004; Gonçalves et al., 2023). These surfactants tend to adsorb onto the rock such like sandstones than anionic surfactants (Kamal et al., 2017; Liu et al., 2021). However, previous work has shown its good performance in carbonate reservoirs (Souraki et al., 2019). Nonionic surfactants do not ionize in water and it has been reported that some nonionic surfactants could be applied under elevated temperature and high salinity conditions (Negin et al., 2017). Commonly applied nonionic surfactants include alkylphenol ethoxylates, poly ethoxylated alcohols and poly propoxylated alcohols (Ahmadi et al., 2012; Bera et al., 2017; Isaac et al., 2022; Sarmah et al., 2020). However nonionic surfactants show relatively poor ability to reduce the IFT compared with other surfactants and it is usually used jointly with other ionic surfactants (Chen et al., 2022a; Chowdhury et al., 2022; Pei et al., 2024). Zwitterionic surfactants contain both anionic and cationic groups therefore exhibiting unique properties for oil production. Betaine type surfactants are the mostly applied zwitterionic surfactant for oil recovery such as carboxyl betaine type and sulfonate betaine type surfactants (Kelleppan et al., 2021; Zhang et al., 2021). It has been reported that zwitterionic surfactants have high temperature and salinity tolerance rendering them an optimal choice for reservoir conditions (Isaac et al., 2024; Kumar and Mandal, 2018). Ultra-low IFT could be achieved by the application of these surfactants as well (Jia et al., 2022; Zhang et al., 2015). Zwitterionic surfactants also demonstrate good compatibility with anionic, cationic and nonionic surfactants (Gbadamosi et al., 2023; Li et al., 2023).

With the continuous development of the reservoir, injection of single surfactant can no longer meet the demand for oil production. Mixture of surfactant and polymer or mixture of different surfactants has been applied to improve the oil recovery efficiency (Kumari et al., 2018; Chen et al., 2022b; Wang et al., 2023b). In particular, mixture of different surfactants has been observed to demonstrate synergistic effect on the oil production process. For instance, it has been reported that the addition of nonionic surfactant to the anionic surfactant reduced the adsorption and lowered the CMC (Kesarwani et al., 2021). The mixture of anionic and nonionic surfactant also achieved lower IFT and better foamability at higher temperature than the individual surfactant (Aziz et al., 2019). The combination of zwitterionic and anionic surfactant could achieve lower IFT promoting the oil displacement efficiency (Kurnia et al., 2020; Ma et al., 2022). Furthermore, viscoelastic behavior was observed for mixed micelles of anionic and zwitterionic surfactants with the presence of NaCl salt (Lopez-Diaz et al., 2005). It was also observed that there is synergistic adsorption of zwitterionic and anionic surfactants thus improving the intensity of the interfacial film (Ma et al., 2022).

Core flooding tests are common practice to examine the performance of individual surfactant or surfactant mixtures for oil displacement efficiency with core plugs (Kesarwani et al., 2021; Ma et al., 2022; Massarweh and Abushaikha, 2023; Wang et al., 2023a). While coreflooding experiments could provide with effective evaluation for the performance of the surfactants, microscale interactions between crude oil, brine, rock and injected surfactants are difficult to observe during coreflooding tests resulting in insufficient understanding of the role of surfactants in enhancing oil recovery. Microfluidic technology enables flexible design of the pore throat architectures and visualization of the fluid flow in pore-scale (Liu et al., 2024a; Zhao et al., 2020). Consequently, various studies on surfactant flooding have been performed using microfluidic devices predominantly micromodels (Yang et al., 2021). For instance, *in situ* emulsification behavior of heavy oil was examined using glass-etching micromodels (Yu et al., 2019). The performance of surfactant and nanoparticles combination was investigated using laser fabricated glass micromodel and polymer-based micromodel (Mohajeri et al., 2019; Liu et al., 2024b). Glass micromodel coated with calcium carbonate nanocrystals was fabricated to emulate calcium carbonate reservoir rock which was subsequently used to evaluate the surfactant performance (Yun et al., 2020). Nevertheless, comprehensive investigation of different surfactant mixtures on the oil recovery performance in pore-scale is still inadequate.

In this study, the performance of anionic-nonionic and anionic-zwitterionic surfactant mixtures with varying ratios in enhancing oil recovery was investigated. Initially, a single dead-end pore structure was extracted from a realistic rock pore structure and employed to rapidly screen the optimal surfactant composition considering the fact that dead-end pore structures are particularly effective in capturing the efficacy of surfactant formulations, especially in displacing trapped oil. Additionally, the impact of connate water on oil recovery efficiency was evaluated. Subsequently, the chemical flooding process was simulated in heterogeneous micromodels using the optimized surfactant mixtures. The microscale displacement process was analyzed by integrating direct observation of fluid flow characteristic, interfacial tension, viscoelasticity, critical micelle concentration, and contact angle measurements. This study offers experimental evidence and a mechanistic understanding of the oil displacement mechanisms associated with different surfactant formulations.

2. Materials and methods

2.1. Fluids

The surfactants employed in this work include sodium dodecyl benzene sulfonate (SDBS), hexyl D-glucoside (APG), and octadecyl dimethyl betaine (BS-18). Chemical structures of the surfactants are shown in Fig. 1. A variety of surfactant mixtures were prepared and the detailed composition is shown in Table 1. Synthetic formation brine was used as the aqueous phase and its composition is presented in Table 2. Crude oil with API° of 31.14, viscosity of 13.92 mPa s and asphaltene content of 5.4% was used as the oil phase.

2.2. Microfluidic setup

Microfluidic devices were fabricated from polydimethylsiloxane (PDMS) using standard photolithography and soft lithography techniques (Duffy et al., 1998). In brief, a silicon wafer with a raised patterned design was created via photolithography. Unpolymerized PDMS was cast onto the silicon wafer and subsequently baked in the oven. Polymerized PDMS was then peeled off and bonded to a glass slide via oxygen plasma treatment thus forming a complete microfluidic device. The experimental setup is depicted in Fig. 2. Fluids were introduced to the

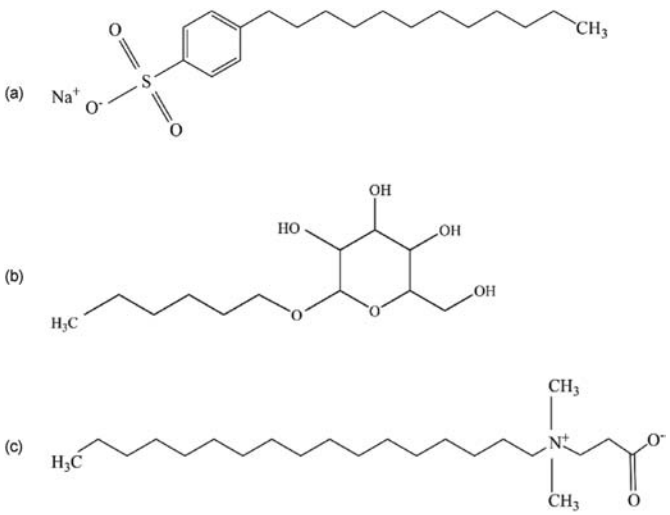


Fig. 1. Chemical structure of (a) SDBS, (b) APG, and (c) BS-18.

Table 1
Composition of surfactant mixtures.

No.	Solution composition	Surfactant conc., mmol/L		
		SDBS	BS-18	APG
1	0.2 wt%SDBS+0.2 wt%BS-18	5.74	5.61	/
2	0.2 wt%SDBS+0.4 wt%BS-18	5.74	11.22	/
3	0.2 wt%SDBS+0.6 wt%BS-18	5.74	16.83	/
4	0.4 wt%SDBS+0.2 wt%BS-18	11.48	5.61	/
5	0.4 wt%SDBS+0.4 wt%BS-18	11.48	11.22	/
6	0.4 wt%SDBS+0.6 wt%BS-18	11.48	16.83	/
7	0.2 wt%SDBS+0.2 wt%APG	5.74	/	7.57
8	0.2 wt%SDBS+0.4 wt%APG	5.74	/	15.13
9	0.2 wt%SDBS+0.6 wt%APG	5.74	/	22.70
10	0.4 wt%SDBS+0.2 wt%APG	11.48	/	7.57
11	0.4 wt%SDBS+0.4 wt%APG	11.48	/	15.13
12	0.4 wt%SDBS+0.6 wt%APG	11.48	/	22.70

Table 2
Composition of the synthetic formation brine.

Total salinity (mg/L)	NaCl(wt%)	$CaCl_2$(wt%)	KCl(wt%)	$MgCl_2$(wt%)
50,000	80	10	7	3

microfluidic device via a syringe pump (LSP02-2A). Microfluidic device was placed under the microscope (BDS400) equipped with a high-speed camera (BR-5002). The high-speed camera was connected to a computer, allowing for real-time observation and recording throughout the experimental process.

2.3. Experimental procedures

2.3.1. Screening of the surfactant composition using microfluidic device with single dead-end pore

A single dead-end pore was designed, as shown in Fig. 3. This simplified dead-end pore structure was extracted from a real rock pore throat structure and it was used to rapidly screen the performance of different surfactant mixtures. Two sets of experiments were conducted to investigate the influence of connate water on the displacement process. In the first set, experiments were carried out in the absence of connate water. The freshly made PDMS device was directly filled with crude oil until a stable oil saturation was achieved. The surfactant mixture was then injected to displace the crude oil until the oil saturation was stabilized. Second set of experiments was performed with the presence of connate water. The PDMS device was initially flushed with formation water, followed by injection of crude oil until the oil saturation was stable. This step established both the connate water saturation and the initial oil saturation. Subsequently, surfactant mixture was injected until the oil saturation was stabilized. The same experimental procedure was repeated for each surfactant mixture tested. Images were taken periodically throughout the entire experiments for further analysis. The displacement efficiency E_{disp} was calculated using the following equation. S_{oi} represents initial oil saturation and S_{or} represents residual oil saturation. Oil saturation was measured using ImageJ software (NIH) for three times. The measurement error was less than 2%.

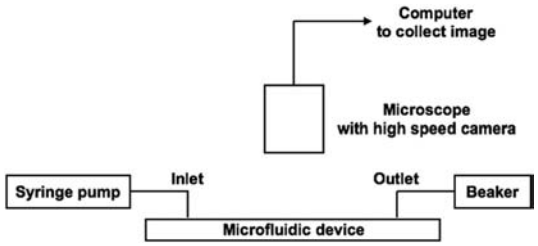


Fig. 2. Schematic of the experimental setup.

$$E_{disp} = \frac{S_{oi} - S_{or}}{S_{oi}} \times 100\% \quad (1)$$

2.3.2. Microscale displacement experiment using heterogeneous micromodels

Microfluidic device with idealized pore-throat network was used to simulate chemical flooding as shown in Fig. 4. The pore-throat network consists of high permeable and low permeable regions. In high permeable region, throat width is 30 μm and length of the square pore is 120 μm. In low permeable region, throat width is 10 μm and length of the square pore is 40 μm. The device was initially saturated with formation brine at a constant rate of 5 μL/min until the saturation was stable. Afterwards crude oil was injected at a constant rate of 2 μL/min until the saturation was stable. Initial oil saturation was installed as a result. Surfactant mixture was injected consequently at a constant rate of 2 μL/min until the oil saturation was stable. Same experimental procedure was repeated using different surfactant mixtures. Images were taken periodically throughout the entire experiments for future analysis. Oil saturation of each image was measured using ImageJ software (NIH). The displacement efficiency was calculated using Eq. (1).

2.3.3. Determination of the interfacial properties, stability and viscosity of the surfactant mixtures

In order to obtain the quantitative interfacial properties between crude oil and surfactant mixtures, interfacial tension (IFT) and viscoelasticity (VE) were measured using rotating droplet tensiometer (CNGTX ENTERPRISES LIMITED, CNGTX600). IFT was measured at a temperature of 30 °C. VE was calculated using the following equation. IFT and VE of each surfactant mixture were measured and calculated.

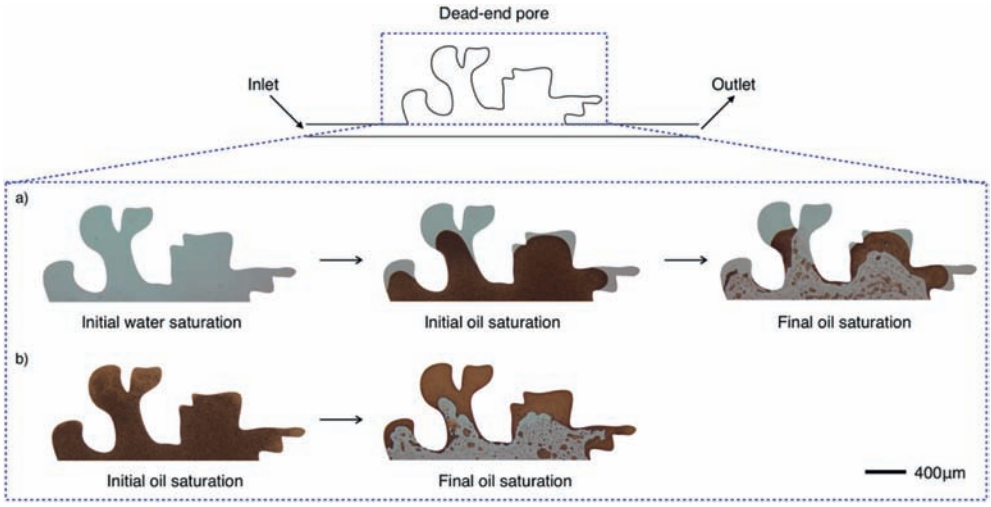


Fig. 3. Schematic of the dead-end pore design and experimental process using dead-end pore a) with the presence of connate water and b) without the presence of connate water.

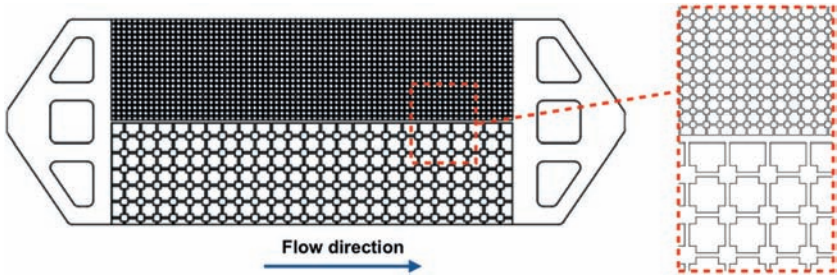


Fig. 4. Schematic of the micromodel design.

$$E^* = \frac{\Delta\gamma}{\Delta A/A_0} \quad (2)$$

where $\Delta\gamma$ is the amplitude of the interfacial tension, ΔA is the amplitude of the surface area and A_0 is the average of the surface area.

The viscosity of surfactant solutions and crude oil was measured using a rotational viscometer (ROTAVISC me-vi Complete) at 170 rpm and 30 °C. The aqueous stability of 12 surfactant solutions with different surfactant concentrations was tested for 8 days at 30 °C. Surfactant solution No.6 and 12 were subject to salinity compatibility tests as well. Surfactants solutions were mixed with formation brine in varying ratios to examine whether precipitation occurs. Aqueous stability of surfactant solutions was examined by visual observation.

2.3.4. Determination of the critical micelle concentration

The critical micelle concentration (CMC) of individual surfactants (SDBS, BS-18, and APG) was first determined by measuring the surface tension at varying surfactant concentrations using the Wilhelmy plate method. The surface tension at different total surfactant concentrations for both anionic-zwitterionic and anionic-nonionic surfactant mixtures was also measured to determine the CMC of the mixed surfactants. Surface tension values were plotted against the logarithm of surfactant concentration, with the inflection point of the curve being identified as the CMC.

2.3.5. Determination of the surface wettability

Glass slides employed for the fabrication of microfluidic devices were aged in crude oil for 2 days. Subsequently, the crude oil was carefully rinsed off from the slides using paraffin prior to conducting the contact angle measurement. The contact angle was determined using the captive drop method with an optical contact angle meter (Krüss DSA100). During this procedure, an oil droplet was affixed beneath the slide in distilled water to obtain the contact angle after oil aging. Afterwards the glass slides were aged in the test solution for 2 days. The measurement process was then repeated to obtain the contact angle after aging in the test solution.

3. Results and discussion

3.1. Interfacial properties and stability of the surfactant mixtures

The stability test results are presented in Table 3. The aqueous surfactant solutions of SDBS and APG, at varying concentrations, remained clear after 8 days. In contrast, the aqueous solutions of SDBS and BS-18 were stable over the 8-day period but exhibited slightly less clarity compared to the mixture of SDBS and APG. In terms of compatibility test in salt, precipitation was only observed when the surfactant mixtures were directly added to a 50,000 ppm brine solution. When the surfactant solution was mixed with formation brine with ratios of 1:1, 2:1 and 3:1, the solutions were cloudy without any precipitation. When the surfactant solution was mixed with formation brine with ratios of 4:1 and 5:1, the solutions were stable and clear.

Table 3
Aqueous stability test of the surfactant mixtures.

Surfactant concentration	Addition of salt	Stability at 30 °C: S (stable), C (cloudy), P (precipitation)
0.2%SDBS+0.2%BS-18	/	S
0.2%SDBS+0.4%BS-18	/	S
0.2%SDBS+0.6%BS-18	/	S
0.4%SDBS+0.2%BS-18	/	S
0.4%SDBS+0.4%BS-18	/	S
0.4%SDBS+0.6%BS-18	50,000 ppm	P
	25,000 ppm (1:1)	C
	16,667 ppm (2:1)	C
	12,500 ppm (3:1)	C
	10,000 ppm (4:1)	S
	8333 ppm (5:1)	S
0.2%SDBS+0.2%APG	/	S
0.2%SDBS+0.4%APG	/	S
0.2%SDBS+0.6%APG	/	S
0.4%SDBS+0.2%APG	/	S
0.4%SDBS+0.4%APG	/	S
0.4%SDBS+0.6%APG	50,000 ppm	P
	25,000 ppm (1:1)	S
	16,667 ppm (2:1)	S
	12,500 ppm (3:1)	S
	10,000 ppm (4:1)	S
	8333 ppm (5:1)	S

IFT and VE for the different surfactant solutions are presented in Table 4. In general, the IFT between SDBS and BS-18 mixture and oil is an order of magnitude lower than that of the SDBS and APG mixture. The VE between SDBS and BS-18 mixture and oil is two orders of magnitude lower than that for the SDBS and APG mixture.

3.2. Critical micelle concentration of the surfactant mixtures

The CMC values for individual surfactant were determined through the surface tension measurements, with the results presented in Fig. 5. As shown in the figure, the CMCs for SDBS, BS-18 and APG are 1.43, 0.06 and 0.15 mmol/L respectively, which are consistent with previously reported CMC values.

The CMCs of both anionic-zwitterionic and anionic-nonionic surfactant mixtures were determined experimentally and the results are presented in Fig. 6. Surface tension was plotted versus the total surfactant concentration on logarithm scale for different mole fractions of SDBS. α_1 represents the mole fraction of SDBS.

According to Rubingh's theory, when two surfactants form mixed micelles in the aqueous phase, the interaction parameter β^M can be calculated using the following equations (Rubingh, 1979).

$$\frac{\left(X_1^M\right)^2 ln\left(\alpha_1 C_{12}^M \Big/ \left(X_1^M C_1^M\right)\right)}{\left(1-X_1^M\right)^2 ln\left[(1-\alpha_1)C_{12}^M \Big/ \left(\left(1-X_1^M\right)C_2^M\right)\right]} = 1 \tag{3}$$

$$\beta^M = \frac{ln\left(\alpha_1 C_{12}^M \Big/ \left(X_1^M C_1^M\right)\right)}{\left(1-X_1^M\right)^2} \tag{4}$$

where X_1^M is the mole fraction of surfactant 1 (SDBS) in the micelles and β^M is the parameter that evaluates the interaction between two surfactants. The value of X_1^M could be obtained by solving Eq. (3) iteratively and was used subsequently to calculate the interaction term β^M. Usually when the value of β^M is positive, there might be antagonism between two surfactants. When the value is negative, synergism between surfactants is implied. The calculation results are shown in Table 5. The interaction parameter β^M for all the surfactant mixtures applied in this work is negative indicating the synergism for both surfactant mixtures.

3.3. Screening of the optimal surfactant composition

3.3.1. Oil displacement in dead-end pore with the presence of connate water

A single dead-end pore structure was employed to screen the optimal surfactant mixture composition. Effect of connate water on oil displacement efficiency was also studied in this work. Oil displacement efficiency was calculated using Eq. (1). The calculated results were demonstrated in Fig. 7a. For the anionic-zwitterionic surfactant mixture, oil displacement efficiency increased with the increase in the total surfactant concentration. It was observed that anionic surfactant contributed more to the oil recovery, as demonstrated by the comparison between experiments where the concentration of BS-18 was kept constant while the concentration of SDBS was increased. However, for anionic-nonionic surfactant mixture as shown in Fig. 7b, an increase in anionic surfactant concentration has a less pronounced effect on the oil displacement efficiency compared to the effect of increasing the nonionic surfactant concentration. Overall, the mixture of 0.4% SDBS+0.6%BS-18 and 0.4%SDBS+0.6%APG yielded relatively higher oil recovery in the dead-end pore with the presence of connate water.

3.3.2. Oil displacement in dead-end pore without the presence of connate water

This set of experiment was conducted without establishing the connate water saturation, meaning that crude oil was in direct

Table 4
Measured interfacial properties of each surfactant mixture.

No.	Surfactant mixture composition	IFT, mN/m	Viscoelasticity, mN/m
1	0.2 wt%SDBS+0.2 wt%BS-18	0.095 ± 0.0158	0.025 ± 0.0086
2	0.2 wt%SDBS+0.4 wt%BS-18	0.117 ± 0.0100	0.027 ± 0.0147
3	0.2 wt%SDBS+0.6 wt%BS-18	0.144 ± 0.0207	0.032 ± 0.0042
4	0.4 wt%SDBS+0.2 wt%BS-18	0.086 ± 0.0036	0.016 ± 0.0015
5	0.4 wt%SDBS+0.4 wt%BS-18	0.104 ± 0.0051	0.027 ± 0.0041
6	0.4 wt%SDBS+0.6 wt%BS-18	0.137 ± 0.0040	0.035 ± 0.0011
7	0.2 wt%SDBS+0.2 wt%APG	1.970 ± 1.2978	1.449 ± 0.1980
8	0.2 wt%SDBS+0.4 wt%APG	2.095 ± 0.0271	3.373 ± 0.9250
9	0.2 wt%SDBS+0.6 wt%APG	1.489 ± 0.0165	1.845 ± 0.6433
10	0.4 wt%SDBS+0.2 wt%APG	2.662 ± 0.3578	5.778 ± 0.6881
11	0.4 wt%SDBS+0.4 wt%APG	0.956 ± 0.0299	7.028 ± 0.4858
12	0.4 wt%SDBS+0.6 wt%APG	0.404 ± 0.0222	4.829 ± 0.1881

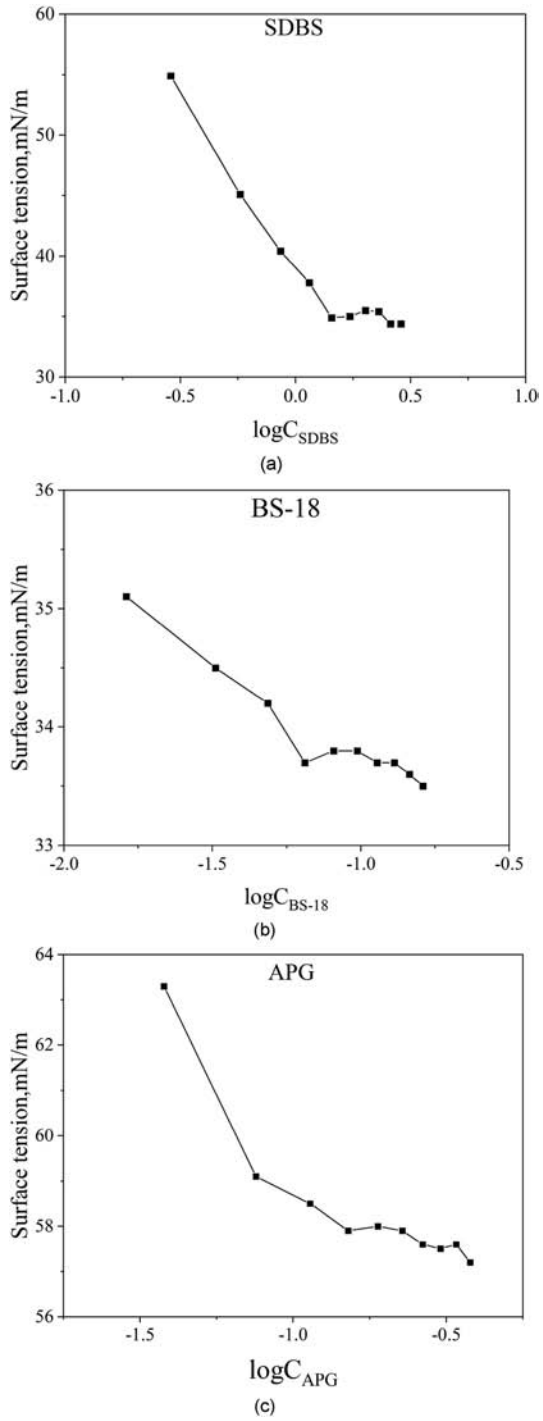


Fig. 5. Measured surface tension versus varying surfactant concentrations for (a) SDBS, (b) BS-18 and (c) APG.

contact with the surface of the pore structure. Compared to the results obtained in the presence of connate water, oil displacement efficiency was relatively lower, as displayed in Fig. 8. For anionic-zwitterionic surfactant mixture, the relationship between surfactant concentration and oil recovery efficiency is similar to that observed with connate water present. The contribution of the anionic surfactant to oil recovery efficiency appeared to be greater than that of the zwitterionic surfactant. With regard to the anionic-nonionic surfactant mixture, oil recovery efficiency demonstrated indistinctive dependence on the surfactant concentration. For anionic-zwitterionic surfactant mixture, 0.4% SDBS+0.4%BS-18 and 0.4%SDBS+0.6%BS-18 exhibited better oil recovery performance in the absence of connate water. For anionic-nonionic surfactant mixture, it was difficult to determine the optimal surfactant composition in the absence of connate water. Without the presence of connate water, crude oil adheres more tightly to the solid surface resulting in relatively lower oil recovery efficiency compared to the experiments conducted in the presence of connate water. In this case, oil removal could be facilitated using surfactant mixtures with stronger interfacial activities. The combination of SDS and BS-18 generally results in lower IFT. The greater absolute value of the interaction parameter β^M for anionic-zwitterionic surfactant mixtures also indicate stronger interaction. Therefore, mixture of SDS and BS-18 with higher concentration particularly those with higher concentration of BS-18 resulted in relatively better oil recovery efficiency. On the other hand, mixtures of nonionic and anionic surfactant exhibit relatively higher interfacial viscoelasticity which could favor the detachment of the crude oil from the solid surface.

In summary, the optimal surfactant composition for both anionic-zwitterionic and anionic-nonionic mixtures was determined on the basis of the screening experimental results obtained using single dead-end pore, both with and without the presence of connate water. Two surfactant mixtures, namely 0.4%SDBS+0.6% BS-18 and 0.4%SDBS+0.6%APG, which demonstrated superior oil recovery efficiency, were selected for further flooding experiments using heterogeneous micromodel.

3.4. Microscale oil displacement in heterogeneous micromodel

A heterogeneous micromodel comprising high and low permeability regions was applied to simulate chemical flooding process. A control experiment was conducted using formation brine. The overall oil recovery efficiency for 0.4%SDBS+0.6%APG, 0.4%SDBS+0.6%BS-18 and formation water were 46.58%, 55.22% and 32.99% respectively. Fig. 9 shows the oil recovery efficiency in both high and low permeability regions. In general, anionic-zwitterionic surfactant mixture exhibited the highest oil recovery efficiency. Specifically, the discrepancy in oil recovery efficiency for the examined surfactant mixtures in high permeability region was not significant. However, in the low permeability zone where the pore and throat sizes are smaller, anionic-zwitterionic surfactant mixture demonstrated notably superior oil recovery performance.

Figs. 10–12 display the final images of the micromodel after flooding experiments demonstrating varying morphology of the residual oil. In the high permeability region, after flooding with 0.4%SDBS+0.6%APG surfactant, the morphology of residual oil could be characterized as a combination of partially clustered oil and dispersed oil droplets in the corners of the pore space as shown in Fig. 10. The residual oil typically exhibited a rounded border with the pore and throat walls largely free of thin oil film attachments. The surface was considered as water-wet, as indicated by the observed wettability state shown in Fig. 10 and measured contact angle shown in Fig. 13. In contrast, after flooding with 0.4%SDBS+0.6%BS-18, fewer oil cluster was observed and solubilized oil in the central region of the pore space was frequently observed. The border of the residual oil differed from that in the previous case, as shown in Fig. 11. The corners of the pore space and the walls of the throats were occupied by the oil phase. A comparison of Figs. 10 and 11 reveals distinct differences in the oil displacement behavior during flooding with anionic-nonionic and anionic-zwitterionic surfactant mixtures. Anionic-nonionic surfactant mixture was observed to displace the oil phase through a peeling-off and mobilization process. Oil slugs were entirely mobilized towards the outlet. Whereas anionic-

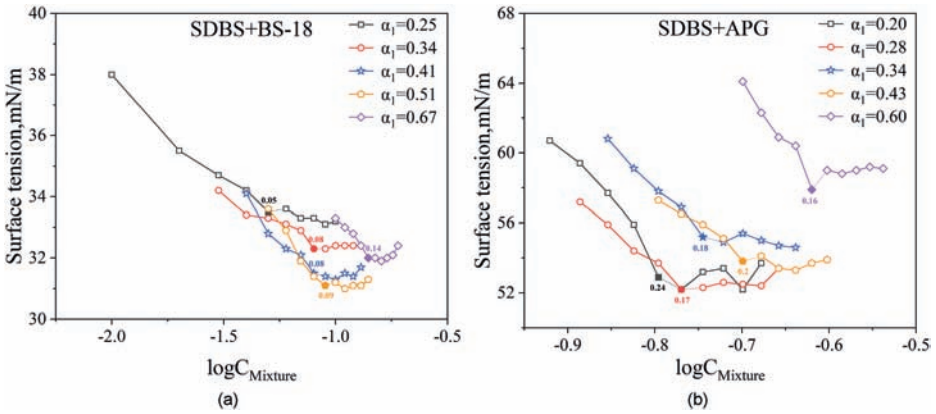


Fig. 6. Measured surface tension versus log surfactant mixture concentrations of a) SDBS and BS-18 and b) SDBS and APG mixtures for different mole fraction of SDBS with marked CMC values.

Table 5
CMCs determined from experiments for different surfactant mixtures at varying mole fraction of SDBS in bulk (α_1), in the mixed micelle (X_1^M) and calculated interaction parameters.

α_1	C_{12}^M (mmol/L)	X_1^M	β^M
SDBS + BS-18			
0.00	0.06	–	–
0.25	0.05	0.212	−5.140
0.34	0.08	0.101	−2.069
0.41	0.08	0.158	−2.722
0.51	0.09	0.190	−2.707
0.67	0.14	0.187	−1.579
1.00	1.43	–	–
SDBS + APG			
0.0	0.15	–	–
0.20	0.16	0.120	−2.165
0.28	0.17	0.147	−2.043
0.34	0.18	0.165	−1.937
0.43	0.19	0.190	−1.756
0.60	0.24	0.269	−1.838
1.00	1.43	–	–

zwitterionic surfactant mixture primarily displaced the oil phase through solubilization and emulsification. Oil slugs were disintegrated into lighter, irregularly shaped oil phases, which were then carried to the outlet. In the control experiment using formation water, as shown in Fig. 12, oil clusters were frequently observed. The corners of the pore space were tightly occupied by the oil phase. Oil film attachment to the throat wall was frequently observed as well. The overall wettability tends to be less water-wet after conventional waterflooding which was also evidenced by the contact angle measurement shown in Fig. 13. Oil solubilization and peeling-off process were rarely observed. Oil displacement behavior in low permeability zone is analogous to that observed in the high permeability zone. Notably, the sweep efficiency of surfactant mixtures was significantly higher than that of the control group in both regions.

3.5. Oil recovery mechanism of different surfactant mixtures

3.5.1. In dead-end pore structure

In the dead-end pore structure, surfactant molecules aggregate at the interface upon contact with crude oil, leading to a reduction in IFT. For the SDBS and BS-18 mixture, W/O emulsions were initially formed upon injection of the surfactant solution. As the surfactant accumulated at the interface, the W/O (indicated by yellow dashed circles) emulsions gradually transitioned to O/W emulsions (indicated by red dashed circles), as shown in Fig. 14. Crude oil was emulsified into smaller droplets and carried along with the flowing surfactant solution. The W/O emulsion diameter ranged approximately from 2 to 76 μm, with the majority of droplets being smaller than 20 μm. The low IFT (10^{-2} to 10^{-1} mN/m) between the SDBS + BS-18 mixture and oil facilitated the emulsification process, resulting in the formation of smaller oil droplets. For the SDBS and APG mixture, as shown in Fig. 15, both W/O (indicated by yellow dashed circles) and O/W (indicated by red dashed circles) emulsions were observed with the presence of

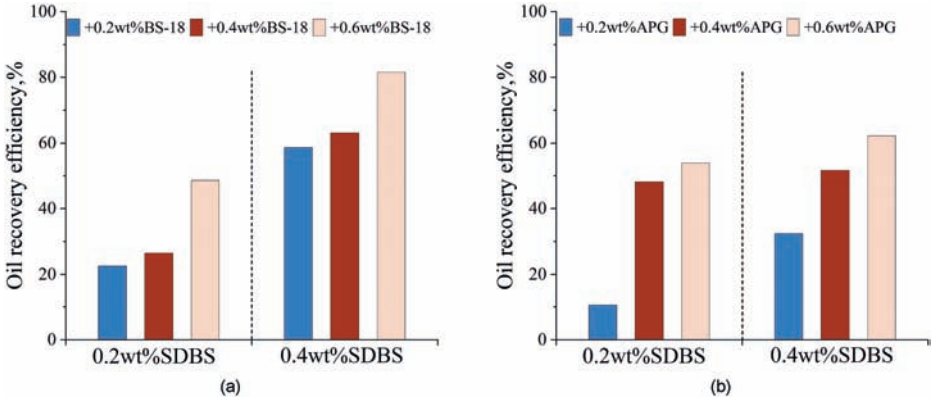


Fig. 7. Oil recovery efficiency of the dead-end pore using (a) anionic-zwitterionic and (b) anionic-nonionic surfactant mixture with the presence of connate water.

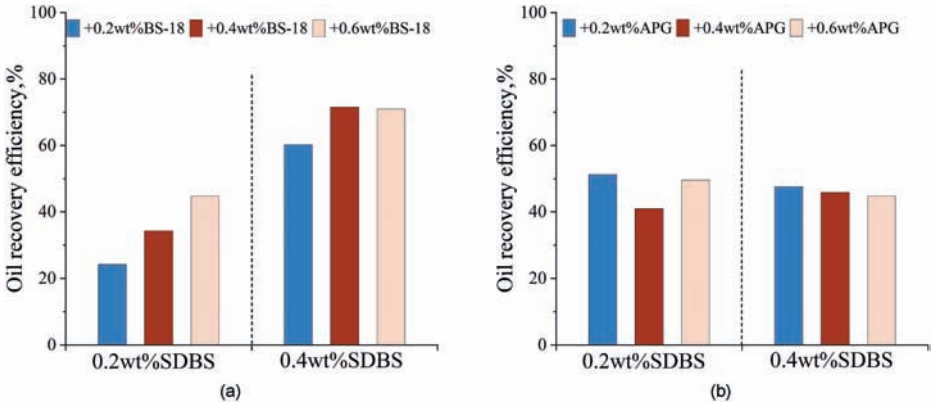


Fig. 8. Oil recovery efficiency of the dead-end pore using (a) anionic-zwitterionic and (b) anionic-nonionic surfactant mixture without the presence of connate water.

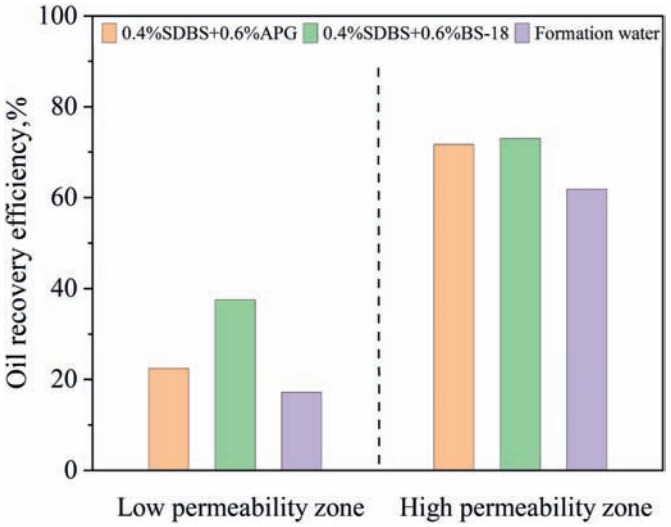


Fig. 9. Oil recovery efficiency in both low and high permeability zone within the micromodel using anionic-nonionic, anionic-zwitterionic surfactant mixtures and formation water.

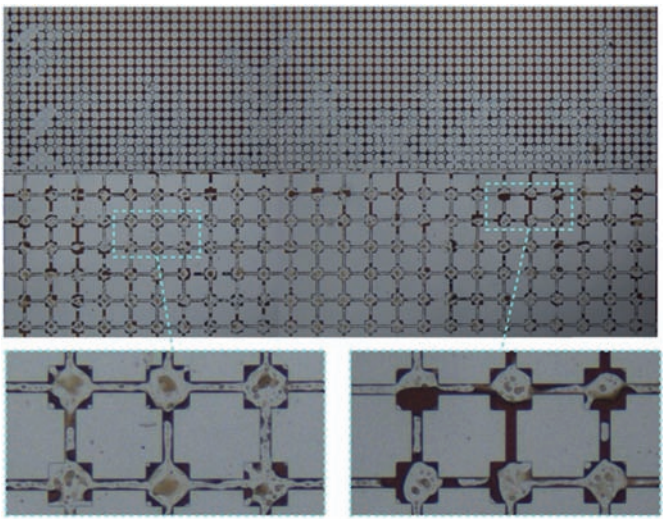


Fig. 11. Final image of the flooding experiment using 0.4% SDBS+0.6%BS-18.

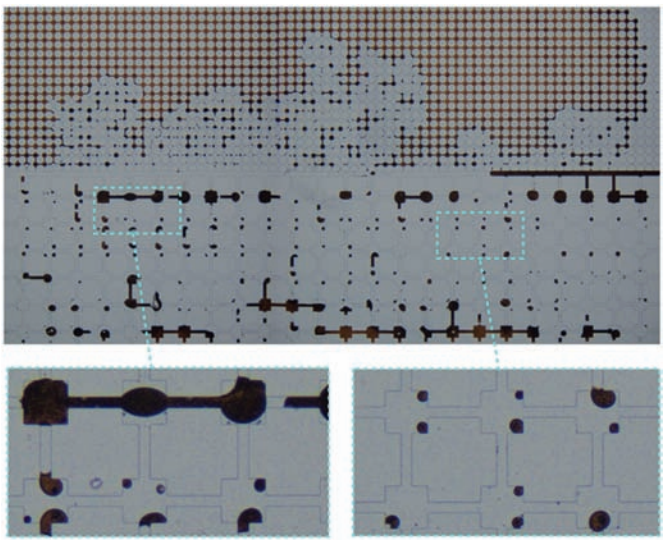


Fig. 10. Final image of the flooding experiment using 0.4% SDBS+0.6%APG.

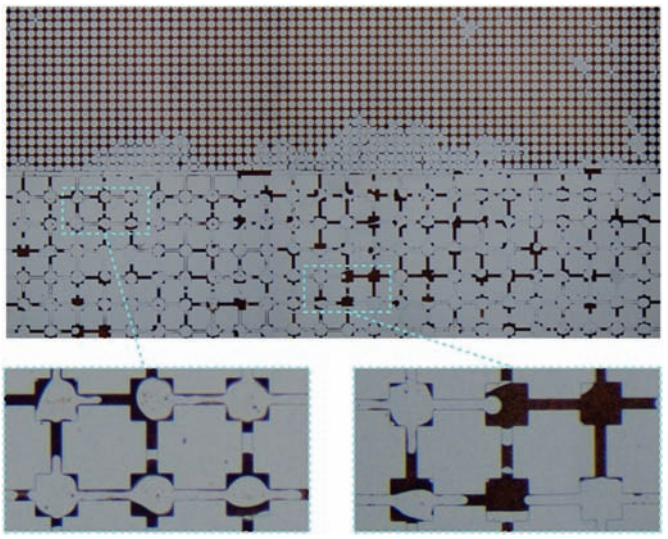


Fig. 12. Final image of the flooding experiment using formation brine.

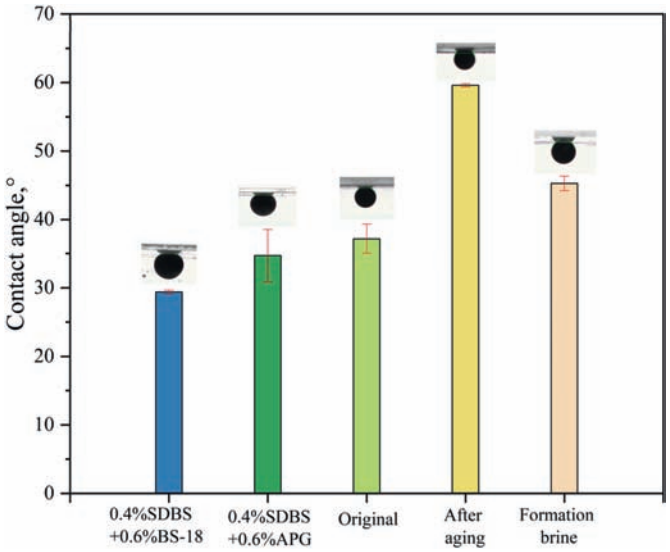


Fig. 13. Contact angle measurement using the selected surfactant formulas and formation brine as the control group.

connate water; however, the emulsion size was larger due to the relatively higher IFT. Despite this, the higher VE between SDBS + APG and crude oil likely contributes to the peel-off and mobilization of the oil phase.

Another observation was that the presence of connate water between oil and solid surface may hinder the removal of oil from the solid surface. By comparing Figs. 14 and 15, it was noted that, in the presence of connate water, thin oil films attached to the solid surface were frequently observed (indicated by black dashed circles). Conversely, oil films were less observed in the absence of connate water, particularly when anionic-nonionic surfactant mixture was used (indicated by blue dashed circles). This phenomenon could be explained by considering the interactions between crude oil, water, and solid surface. According to the Derjaguin, Landau, Verwey, and Overbeek (DLVO) theory (Derjaguin, 1941; Verwey, 1947), the overall interaction F can be calculated using the following equations:

$$F = F_{dl} + F_{vdw} \tag{5}$$

where F_{dl} is the repulsive interaction and F_{vdw} is the attractive interaction. These two terms are expresses as follows (Smith et al., 2020):

$$\frac{F_{dl}}{R} = 4\pi\varepsilon_0\varepsilon k\varphi^2 e^{-kh} \tag{6}$$

$$\frac{F_{vdw}}{R} = -\frac{A}{6h^2} \tag{7}$$

where R is the effective radius, φ is the effective potential, ε is the dielectric constant of the solution, ε_0 is the dielectric permittivity in a vacuum, h is the separation distance, A is the Hamaker constant and k is the effective decay parameter which agrees with the reciprocal of the Debye length κ^{-1} which is expressed in Eq. (8).

$$\kappa = \left(\frac{2q^2 I}{\varepsilon_0\varepsilon N_A KT}\right)^{1/2} \tag{8}$$

where q is the elementary charge, I is the ionic strength, N_A is the Avogadro's constant, K is the Boltzmann constant and T is the absolute temperature. The repulsion between two surfaces is dependent upon the Debye length, which is influenced by the interfacial potential and ionic strength of the solution or the bulk concentration of the electrolyte. The presence of high salinity formation water between oil and solid surface reduces the Debye length, resulting in smaller repulsion. The van der Waals attraction, however, is less affected by the bulk concentration of the electrolyte, as described by Eq. (7). Water is regarded as a polar molecule whereas oil is considered as a nonpolar molecule. The solid surface of the device used in this study can become charged upon contact with an aqueous solution. The attraction between polar molecules and a charged solid surface is stronger than the attraction between polar and nonpolar molecules. Therefore, the presence of high salinity water film between crude oil and solid surface results in lower repulsion and a higher degree of attraction compared to the situation without high salinity connate water. As a result, oil film attachment to the solid surface was more frequently observed in the presence of connate brine.

3.5.2. In heterogeneous micromodel

Microscale displacement experiments were conducted to investigate the performance of various surfactant mixtures in a heterogeneous micromodel. The measured viscosities of 0.4% SDBS+0.6%BS-18 and 0.4%SDBS+0.6%APG surfactant mixtures were both 1.32 mPa s. Therefore, viscosity of the displacing fluid is not considered as a significant influencing factor in this study. As a result, the oil displacement mechanisms are presumably dependent on the interfacial properties between the surfactant mixtures and crude oil. The application of anionic-zwitterionic surfactant mixture resulted in strong emulsification and possible solubilization of the crude oil, as illustrated in Fig. 11. Both O/W and W/O emulsions were observed in both high and low permeability regions. The continuous oil phase was emulsified into small oil droplets that could be easily mobilized. Furthermore, solubilization of the oil phase was observed, as evidenced by the lighter brown color at the boundary between oil and surfactant solution,

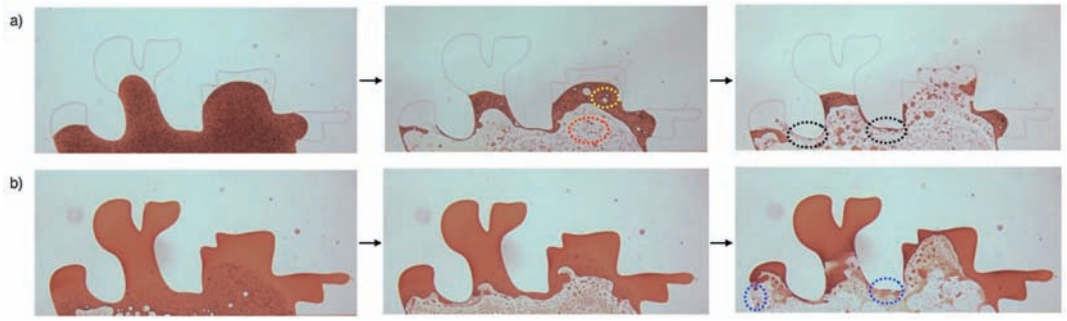


Fig. 14. Time sequenced images during injection of 0.4% SDBS+0.6%BS-18 a) with and b) without the presence of connate water.

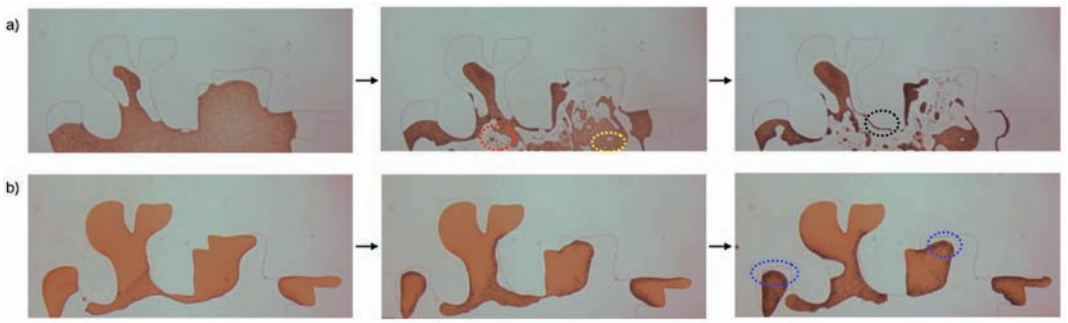


Fig. 15. Time sequenced images during injection of 0.4% SDBS+0.6%APG a) with and b) without the presence of connate water.

or within the middle of the pore structure. In the case of the anionic-nonionic surfactant mixture, O/W and W/O emulsions with larger diameter were observed yet the solubilization of the crude oil was not evident. Nevertheless, this surfactant combination facilitated the removal of the oil from the surface of the pore structure. This discrepancy in oil displacement behavior is presumably attributed to differences in IFT, VE and CMC of the surfactant mixture. First of all, the IFT values of anionic-zwitterionic surfactant mixture are an order of magnitude lower than those of anionic-nonionic surfactant mixture. The calculated CMC values for the surfactant mixtures further reveal that the CMCs of the anionic-zwitterionic surfactant mixture are lower than those of the anionic-nonionic surfactant mixture. Additionally, the interaction parameter β^M indicates a stronger synergistic effect for the anionic-zwitterionic surfactant mixture. The negatively charged head of SDBS and the positively charged head of BS-18 facilitate more compact packing at the interface, whereas the larger head of the nonionic surfactant APG results in a less compact arrangement of SDBS and APG molecules at the interface. The denser packing of SDBS and BS-18 molecules enhances micelle formation and solubilization of crude oil, as demonstrated in Fig. 16. The concentration of the anionic-zwitterionic surfactant mixture applied in this study is well above the CMC, making micellar solubilization a potential factor in enhancing oil recovery. Previous studies have also suggested that micellar solubilization serves as a supplementary mechanism for surfactant-based enhanced oil recovery at low surfactant concentrations (Gong et al., 2020). In addition, the VE values of anionic-nonionic surfactant mixture are higher than those of the anionic-zwitterionic surfactant mixture. Higher VE between oil and water interface contributes to maintaining a more continuous oil phase. As a result, crude oil could be more effectively stripped off from the solid surface.

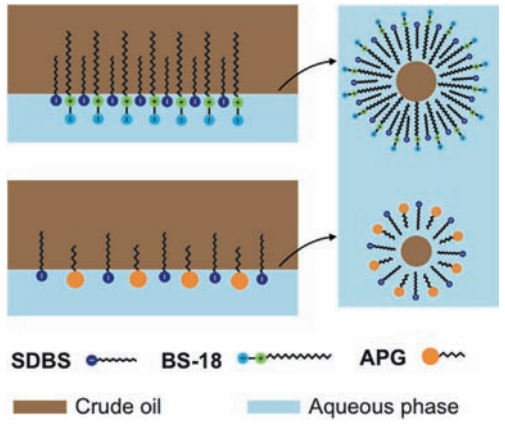


Fig. 16. Schematic of different surfactant mixtures at the interface and micellar solubilization.

4. Conclusions

This work investigated the performance of anionic-nonionic and anionic-zwitterionic surfactant mixtures on the oil displacement efficiency. The properties of surfactant mixtures, including interfacial tension, viscoelasticity and critical micelle concentration, were comprehensively examined. Single dead-end pore structure was firstly employed to screen for the optimal surfactant mixture composition, and the impact of connate water on oil recovery was also investigated. 0.4%SDBS+0.6%BS-18 and 0.4% SDBS+0.6%APG surfactant mixtures were selected on account of higher oil recovery efficiency. The oil displacement performance of the selected surfactant mixtures was further examined using heterogeneous micromodel consisting of high and low permeable regions. 0.4%SDBS+0.6%BS-18 mixture resulted in higher oil recovery in both low and high permeability regions. Oil recovery mechanism of different surfactant mixture was investigated. The anionic-zwitterionic surfactant mixture displaced oil majorly through emulsification and micellar solubilization, owing to its lower interfacial tension and lower critical micelle concentration. In contrast, the anionic-nonionic surfactant mixture displaced oil mainly through peeling-off and mobilization process, driven by its relatively higher interfacial tension and viscoelasticity between oil and surfactant. Additionally, the presence of connate water was found to promote the attachment of oil film to the solid surface, which may be attributed to the different interactions between oil-solid, water-oil and water-solid interfaces. Overall, this study provides a comprehensive evaluation of the performance of anionic-zwitterionic and anionic-nonionic surfactant mixtures on the microscale oil recovery process, elucidating the microscopic interactions between crude oil, surfactant mixtures and formation brine. The experimental results and proposed mechanisms offer valuable insights into the optimal application of surfactant mixtures for various oil recovery scenarios.

CRediT authorship contribution statement

Yafei Liu: Writing – review & editing, Writing – original draft, Supervision, Investigation, Funding acquisition, Conceptualization. **Chenyue Ling:** Writing – original draft, Methodology, Formal analysis, Data curation. **Yixin Luo:** Methodology, Investigation. **Na Liu:** Data curation. **Gaoxin Li:** Formal analysis. **Desheng Zhou:** Supervision.

Declaration of competing interest

The authors declare that they have no known competing financial interests or personal relationships that could have appeared to influence the work reported in this paper.

Acknowledgements

This work was supported by the National Natural Science Foundation of China (Grant No. 52174028 and U23B2089) and Innovation Capability Support Program of Shaanxi (Program No. 2023KJXX-051).

References

Ahmadi, M.A., Zendehboudi, S., Shafiei, A., James, L., 2012. Nonionic surfactant for enhanced oil recovery from carbonates: adsorption kinetics and equilibrium. Ind. Eng. Chem. Res. 51 (29), 9894–9905.

Aziz, U.A., Adnan, N., Sohri, M., Mohshim, D.F., Idris, A.K., Azman, M.A., 2019. Characterization of anionic–nonionic surfactant mixtures for enhanced oil recovery. J. Solut. Chem. 48 (11), 1617–1637.

Bashir, A., Haddad, A.S., Rafati, R., 2022. A review of fluid displacement mechanisms in surfactant-based chemical enhanced oil recovery processes: analyses of key influencing factors. Pet. Sci. 19 (3), 1211–1235.

Bera, A., Mandal, A., Belhaj, H., Kumar, T., 2017. Enhanced oil recovery by nonionic surfactants considering micellization, surface, and foaming properties. Pet. Sci. 14 (2), 362–371.

Bi, Z., Liao, W., Qi, L., 2004. Wettability alteration by CTAB adsorption at surfaces of SiO2 film or silica gel powder and mimic oil recovery. Appl. Surf. Sci. 221 (1), 25–31.

Chen, S., Han, M., AlSofi, A.M., Fahmi, M.M., 2022a. Experimental evaluation of non-ionic mixed surfactant formulations at high-temperature and high-salinity conditions. J. Petrol. Sci. Eng. 219, 111084.

Chen, W., Schechter, D.S., 2021. Surfactant selection for enhanced oil recovery based on surfactant molecular structure in unconventional liquid reservoirs. J. Petrol. Sci. Eng. 196, 107702.

Chen, X., Sotomayor, M., Alshaer, H.J., Song, H., Panthi, K., Balhoff, M., Mohanty, K. K., 2022b. Enhanced oil recovery with anionic and zwitterionic surfactants in carbonate rocks: a CT-aided investigation. Fuel 311, 122589.

Chowdhury, S., Shrivastava, S., Kakati, A., Sangwai, J.S., 2022. Comprehensive review on the role of surfactants in the chemical enhanced oil recovery process. Ind. Eng. Chem. Res. 61 (1), 21–64.

Derjaguin, B.V., 1941. Theory of the stability of strongly charged lyophobic sol and of the adhesion of strongly charged particles in solutions of electrolytes. Acta Phys. Chim. 14, 633.

Duffy, D.C., McDonald, J.C., Schueller, O.J., 1998. Whitesides GM. Rapid prototyping of microfluidic systems in poly(dimethylsiloxane). Anal. Chem. 70 (23), 4974–4984.

Elraies, K.A., Tan, I.M., Awang, M., Saaid, I., 2010. The synthesis and performance of sodium methyl ester sulfonate for enhanced oil recovery. Petrol. Sci. Technol. 28 (17), 1799–1806.

Fu, B., Liu, R., Gao, S., 2024. Unlocking the mechanism of unique interfacial behavior and highly efficient oil displacement of amphiphilic carbon nanosheets. Energy Fuel. 38 (20), 19442–19454.

Gbadamosi, A., Hussai, S.M.S., Kamal, M.S., Patil, S., Solling, T., Hassan, S.F., Wang, J., 2023. Evaluating the potential of zwitterionic surfactants for enhanced oil recovery: effect of headgroups and unsaturation. Energy Fuel. 37 (7), 5078–5086.

Gonçalves, R.A., Holmberg, K., Lindman, B., 2023. Cationic surfactants: a review. J. Mol. Liq. 375, 121335.

Gong, L., Liao, G., Luan, H., Chen, Q., Nie, X., Liu, D., Feng, Y., 2020. Oil solubilization in sodium dodecylbenzenesulfonate micelles: new insights into surfactant enhanced oil recovery. J. Colloid Interface Sci. 569, 219–228.

Hama, S.M., Manshad, A.K., Ali, J.A., 2023. Review of the application of natural surfactants in enhanced oil recovery: state-of-the-art and perspectives. Energy Fuel. 37 (14), 10061–10086.

Hirasaki, G.J., Miller, C.A., Puerto, M., 2011. Recent advances in surfactant EOR. SPE J. 16 (4), 889–907.

Isaac, O.T., Pu, H., Oni, B.A., Samson, F.A., 2022. Surfactants employed in conventional and unconventional reservoirs for enhanced oil recovery—A review. Energy Rep. 8, 2806–2830.

Isaac, O.T., Samson, F.A., Pu, H., Oni, B.A., Ogunkunle, T.F., Tomomewo, O.S., Nkok, L. Y., 2024. Experimental investigation of zwitterionic surfactant for enhanced oil recovery in unconventional reservoir: a study in the middle bakken formation. Colloids Surf. A Physicochem. Eng. Asp., 134768

Jia, R., Kang, W., Li, Z., Yang, H., Gao, Z., Zheng, Z., Yang, H., Zhou, B., Jiang, H., Turtabayev, S., 2022. Ultra-low interfacial tension (IFT) zwitterionic surfactant for imbibition enhanced oil recovery (IEOR) in tight reservoirs. J. Mol. Liq. 368, 120734.

Kamal, M.S., Hussein, I.A., Sultan, A.S., 2017. Review on surfactant flooding: phase behavior, retention, IFT, and field applications. Energy Fuel. 31 (8), 7701–7720.

Kelleppan, V.T., King, J.P., Butler, C.S.G., Williams, A.P., Tuck, K.L., Tabor, R.F., 2021. Heads or tails? The synthesis, self-assembly, properties and uses of betaine and betaine-like surfactants. Adv. Colloid Interface Sci. 297, 102528.

Kesarwani, H., Saxena, A., Mandal, A., Sharma, S., 2021. Anionic/nonionic surfactant mixture for enhanced oil recovery through the investigation of adsorption, interfacial, rheological, and rock wetting characteristics. Energy Fuel. 35 (4), 3065–3078.

Ko, K.M., Chon, B.H., Jang, S.B., Jang, H.Y., 2014. Surfactant flooding characteristics of dodecyl alkyl sulfate for enhanced oil recovery. J. Ind. Eng. Chem. 20 (1), 228–233.

Kralova, I., Sjöblom, J., 2009. Surfactants used in food industry: a review. J. Dispersion Sci. Technol. 30 (9), 1363–1383.

Kumar, A., Mandal, A., 2018. Characterization of rock-fluid and fluid-fluid interactions in presence of a family of synthesized zwitterionic surfactants for application in enhanced oil recovery. Colloids Surf. A Physicochem. Eng. Asp. 549, 1–12.

Kumari, R., Kakati, A., Nagarajan, R., Sangwai, J.S., 2018. Synergistic effect of mixed anionic and cationic surfactant systems on the interfacial tension of crude oil-water and enhanced oil recovery. J. Dispersion Sci. Technol. 40 (7), 969–981.

Kurnia, I., Zhang, G., Han, X., Yu, J., 2020. Zwitterionic-anionic surfactant mixture for chemical enhanced oil recovery without alkali. Fuel 259, 116236.

Li, L., Sun, Y., Liu, J., Wang, Z., Wu, Y., Zhao, M., Dai, C., 2023. Zwitterionic-nonionic compound surfactant system with low chromatographic separation effect for enhanced oil recovery. J. Mol. Liq. 390, 123004.

Liu, Y., He, F., Hu, Z., Zhu, Z., Ling, C., 2024a. Microfluidic study on the effect of single pore–throat geometry on spontaneous imbibition. Langmuir 40 (36), 19209–19219.

Liu, Y., Liu, Z., Wang, Y., Hu, Z., Zhu, Z., Jie, Y., 2024b. Effect of different surfactants and nanoparticles on pore-scale oil recovery process using heterogeneous micromodel. Int. J. Energy Res. 2024 (1), 5319748.

Liu, Z., Zhao, G., Brewer, M., Lv, Q., Sudhölter, E.J., 2021. Comprehensive review on surfactant adsorption on mineral surfaces in chemical enhanced oil recovery. Adv. Colloid Interface Sci. 294, 102467.

Lopez-Diaz, D., Garcia-Mateos, I., Velázquez, M.M., 2005. Synergism in mixtures of zwitterionic and ionic surfactants. Colloids Surf. A Physicochem. Eng. Asp. 270, 153–162.

Ma, H., Ranimol, S., Cameron, A., 2022. Synergetic system of zwitterionic/anionic surfactants with ultralow interfacial tension and high salt resistance for enhancing heavy oil recovery. Energy Fuel. 36 (15), 8216–8223.

Massarweh, O., Abushaikha, A.S., 2023. Application of surfactants in enhancing oil recovery from tight carbonates: physicochemical properties and core flooding experiments. Geoenergy Sci. Eng. 221, 211400.

Mohajeri, M., Rasaei, M.R., Hekmatzadeh, M., 2019. Experimental study on using SiO2 nanoparticles along with surfactant in an EOR process in micromodel. Petrol. Res. 4 (1), 59–70.

Mulligan, C.N., Yong, R.N., Gibbs, B.F., 2001. Surfactant-enhanced remediation of contaminated soil: a review. Eng. Geol. 60 (1–4), 371–380.

Negin, C., Ali, S., Xie, Q., 2017. Most common surfactants employed in chemical enhanced oil recovery. Petroleum 3 (2), 197–211.

Pei, H., Liu, Y., Shan, J., Zhao, J., Zhang, J., Wu, Y., Zhang, G., 2024. Enhancement of in-situ emulsification performance through the synergistic effects of zwitterionic and nonionic-anionic surfactants to improve heavy oil recovery. J. Mol. Liq. 410, 125562.

Quintero, L., 2002. An overview of surfactant applications in drilling fluids for the petroleum industry. J. Dispersion Sci. Technol. 23 (1–3), 393–404.

Rubingh, D.N., 1979. Mixed Micelle Solutions. Springer, pp. 337–354.

Sarmah, S., Gogoi, S.B., Xianfeng, F., Baruah, A.A., 2020. Characterization and identification of the most appropriate nonionic surfactant for enhanced oil recovery. J. Pet. Explor. Prod. Technol. 10, 115–123.

Singh, A., Van Hamme, J.D., Ward, O.P., 2007. Surfactants in microbiology and biotechnology: part 2. Application aspects. Biotechnol. Adv. 25 (1), 99–121.

Smith, A.M., Borkovec, M., Trefalt, G., 2020. Forces between solid surfaces in aqueous electrolyte solutions. Adv. Colloid Interface Sci. 275, 102078.

Souraki, Y., Hosseini, E., Yaghodous, A., 2019. Wettability alteration of carbonate reservoir rock using amphoteric and cationic surfactants: experimental investigation. Energy Sources, Part A Recovery, Util. Environ. Eff. 41 (3), 349–359.

Tavakkoli, O., Kamyab, H., Shariati, M., Mohamed, A.M., Junin, R., 2022. Effect of nanoparticles on the performance of polymer/surfactant flooding for enhanced oil recovery: a review. Fuel 312, 1–14.

Vecino, X., Cruz, J.M., Moldes, A.B., Rodrigues, L.R., 2017. Biosurfactants in cosmetic formulations: trends and challenges. Crit. Rev. Biotechnol. 37 (7), 911–923.

Verwey, E.J.W., 1947. Theory of the stability of lyophobic colloids. J. Phys. Chem. 51 (3), 631–636.

Wang, F., Wang, L., Jiao, L., Liu, Z., Yang, K., 2023a. Experimental mechanism for enhancing oil recovery by spontaneous imbibition with surfactants in a tight sandstone oil reservoir. Energy Fuel. 37 (12), 8180–8189.

Wang, Z., Dai, C., Liu, J., Dong, Y., Liu, J., Sun, N., Li, L., 2023b. Anionic-nonionic and nonionic mixed surfactant systems for oil displacement: impact of ethoxylate chain lengths on the synergistic effect. Colloids Surf. A Physicochem. Eng. Asp. 678, 132436.

Yang, W., Lu, J., Wei, B., Yu, H., Liang, T., 2021. Micromodel studies of surfactant flooding for enhanced oil recovery: a review. ACS Omega 6 (9), 6064–6069.

Yu, F., Jiang, H., Fan, Z., Xu, F., Su, H., Li, J., 2019. Formation and flow behaviors of *in situ* emulsions in heavy oil reservoirs. Energy Fuel. 33 (7), 5961–5970.

Yun, W., Chang, S., Cogswell, D.A., Eichmann, S.L., Wang, W., 2020. Toward Reservoir-on-a-Chip: rapid performance evaluation of enhanced oil recovery surfactants for carbonate reservoirs using a calcite-coated micromodel. Sci. Rep. 10 (1), 782.

Zhang, Q.Q., Cai, B.X., Xu, W.J., Gang, H.Z., Liu, J.F., Yang, S.Z., Mu, B.Z., 2015. Novel zwitterionic surfactant derived from Castor oil and its performance evaluation for oil recovery. Colloids Surf. A Physicochem. Eng. Asp. 483, 87–95.
Zhang, Y., Mao, J., Zhao, J., Liao, Z., Xu, T., Mao, J., Sun, H., Zheng, L., Ni, Y., 2021. Synergy between different sulfobetaine-type zwitterionic gemini surfactants: surface tension and rheological properties. J. Mol. Liq. 332, 115141.
Zhao, X., Feng, Y., Liao, G., Liu, W., 2020. Visualizing in-situ emulsification in porous media during surfactant flooding: a microfluidic study. J. Colloid Interface Sci. 578, 629–640.
Zhao, Z., Liu, F., Qiao, W., Li, Z., Cheng, L., 2006. Novel alkyl methylnaphthalene sulfonate surfactants: a good candidate for enhanced oil recovery. Fuel 85 (12), 1815–1820.